Journal of Ovonic Research Vol. 18, No. 1, January - February 2022, p. 21- 28

Shell-model calculations of the spectroscopic properties of neutron-rich calcium isotopes around ^{40,48}Ca cores

I. L. Benchikh[a,*], L. Aissaoui[b]

[a] *Information Processing and Telecommunication Laboratory, Department of Electrical Engineering, Faculty of Technology, University TAHRI Mohammed Bechar, Algeria*

[b] *Physics of Radiations and their Interaction with Matter Laboratory, Department of Physics, Faculty of Matter Sciences, University of Batna 1, Batna, Algeria*

With the aim of predicting the possible existence of new magic numbers, we theoretically studied the recently available experimental data for spectroscopic properties of the neutron rich even-even calcium isotopes around ^{40,48}Ca doubly magic cores. The calculations were performed with the phenomenological interactions for *fppn* and *HO* model spaces using the nuclear structure code Nushell. The two-body matrix elements (TBMEs) of the new effective interaction KB3G48 were derived from the microscopic Kuo-Brown's G-matrix interaction KB3GPN for ^{40}Ca core. The calculated energies $E(2_1^+)$ of the first excited state, the ratio $R_{4/2}$ of the excitation energies, the reduced electric transition probabilities $B(E2;\ 2_1^+ \rightarrow 0_1^+)$ and the ratio $B_{4/2}$ of reduced transition probabilities are compared with the available experimental data. The results of this study are an attempt to demonstrate that $N = 32$ or $N = 34$ are new magic numbers for Ca isotopes.

(Received May 10, 2021; Accepted January 12, 2022)

Keywords: Nushell code, KB3GPN and KB3G48 interactions, $E(2_1^+)$ energies, $B(E2)$ reduced transition probabilities, $R_{4/2}$ and $B_{4/2}$ ratios

1. Introduction

The existence of the magic numbers was one of the empirical evidences for the development of the nuclear shell model [1], and an ideal probe to test our knowledge of nuclear interactions by comparing experimental data with shell-model predictions [2, 3]. The magic numbers were suggested by Mayer and Jensen [4, 5] and have remained valid for the mass region near to the valley of β-stability. Nuclei with magic numbers are characterized by a quasi-spherical shape, high energies $E(2_1^+)$ of the first excited states and also reduced transition probabilities $B(E2;\ 2_1^+ \rightarrow 0_1^+)$. The influence of these numbers is changed for nuclei far from the valley of β-stability. These magic numbers have been put into question, with their disappearance for neutron-rich nuclei around $N = 20$ [6] and $N = 28$ [7, 8], but also with the appearance at $N = 32,\ 34$ new magic numbers.

Recently, neutron-rich *fp*-shell nuclei have received much attention on both experimental and theoretical fronts with the possibility of new sub-shell closures at $N = 32$ and 34. The magicity at $N = 32$ was signed from the measurements of reduced transition probabilities $B(E2;\ 2_1^+ \rightarrow 0_1^+)$ and the $E(2_1^+)$ energies in ^{50}Ar [9], ^{52}Ca [10, 11] ^{54}Ti [12-15], and ^{56}Cr [16, 17] and further confirmed by high-precision mass measurements of exotic isotopes ^{52}Ca and ^{52}K [11, 18]. More recently, a strong sub-shell closure at $N = 32$ has also been indicated in $^{52-54}$Sc isotopes using direct mass measurement, which has proved to be quenched in $^{52-55}$V isotopes [19, 20]. The magicity at $N = 34$ was suggested in ^{54}Ca [21, 22] and in ^{52}Ar [23], and theoretically supported by *ab*-initio calculations [24, 25] and shell models [9, 21]. Very recently, the mass

*Corresponding author: bencheikh.iftikhar@univ-bechar.dz
https://doi.org/10.15251/JOR.2022.181.21

evolution in calcium isotopes beyond $N = 34$ has again indicated the magicity at $N = 34$ [26]. On the other hand, the theoretical calculations made for *fp*-shell nuclei in calcium isotopes with the phenomenological interactions FPD6 [27] and KB3GPN [28] revealed a significant gap in the shell at ^{52}Ca ($N = 32$). However, the phenomenological interaction GX1APN [29] did not show this shell gap.

In the following sections, we report the details and the results of the present calculations of such spectroscopic parameters of neutron-rich $^{50-58}$Ca isotopes in *fp*-shell by using the nuclear shell model with ^{40,48}Ca cores. These calculations are performed by means of the nuclear structure code Nushell [3].

2. Calculation details

Shell model calculations were performed for the neutron rich nuclei even-even Ca isotopes in mass region $A = 50\text{–}58$. In order to accomplish these calculations, we have carried out two sets of calculations using Nushell code [3]. In the first set, valence space is $\pi\nu(fp) \equiv fppn$ shell that comprises $\pi(1f_{7/2}, 2p_{3/2}, 1f_{5/2}, 2p_{1/2})$ and $\nu(1f_{7/2}, 2p_{3/2}, 1f_{5/2}, 2p_{1/2})$ for proton and neutron orbits, and treating ${}^{40}_{20}Ca$ as the core. The second set of calculations has been performed in $\pi(f_{7/2}) - \nu(pf) \equiv HO$ valence space includes the orbit $\pi(1f_{7/2})$ for protons and $\nu(2p_{3/2}, 1f_{5/2}, 2p_{1/2})$ for neutrons by taking ${}^{48}_{20}Ca$ as the core.

The *fppn* model space calculations are carried out using the KB3GPN and GX1APN interactions in the proton-neutron formalism with ${}^{40}_{20}Ca$ core [28, 29]. The KB3GPN interaction is the latest modified version of KB3 interactions [30], which is obtained on the basis of the microscopic Kuo-Brown's G-matrix interaction [31], with various monopole corrections. Both these interactions are quite successful in the lower *fp*-shell ($A \leq 52$). The GX1APN interaction is a modified version of GX1 interaction by Honma *et al.*, [32] which is derived from a microscopic calculation by Hjorth-Jensen based on renormalized G-matrix theory with the Bonn-C nucleon-nucleon interaction [33]. It is obtained by modifying 70 well-determined linear combinations of four single particle energies (SPEs) and 195 two-body matrix elements (TBMEs) by iterative fitting calculations to about 700 experimental energy data out of 87 nuclei from $A = 47$ to $A = 66$. The single-particle energies for KB3GPN [31,34,35] and GX1APN [32,36] interactions are listed in Table 1. These SPE values correspond to both single-neutron and single-proton states. Note that single-neutron energies of $2p_{3/2}$, $2p_{1/2}$ and $1f_{5/2}$ states in ${}^{41}_{20}Ca$ are usually obtained only by some calculations after averaging over spectroscopic factors in the $^{40}Ca(d,p)^{41}Ca$ reaction. By using the data in the ENSDF and Atomic Mass Data Center files [37], the single-neutron energies results are follows: $\varepsilon_{\upsilon 2p_{3/2}} \approx -6.00$, $\varepsilon_{\upsilon 1f_{5/2}} \approx -1.52$, $\varepsilon_{\upsilon 2p_{1/2}} \approx -4.00$, $\varepsilon_{\upsilon 1f_{7/2}} \approx -8.363$ and $\varepsilon_{\pi 1f_{7/2}} \approx -1.085$. These values are more or less close to those presented in Table 1, which however are different from each other.

Table 1. Single-particle energies (in MeV) for KB3GPN and GX1APN interactions.

Orbits	KB3GPN	GX1APN
$1f_{7/2}$	-8.6000	-8.6240
$2p_{3/2}$	-6.6000	-5.6793
$1f_{5/2}$	-2.1000	-1.3829
$2p_{1/2}$	-4.6000	-4.1370

Table 2. Single-particle energies (in MeV) for HO and KB3G48 interactions.

Orbits	HO	KB3G48
$\pi 1f_{7/2}$	-9.628	-9.625
$\upsilon 2p_{3/2}$	-5.144	-5.146
$\upsilon 1f_{5/2}$	-1.186	-1.561
$\upsilon 2p_{1/2}$	-3.116	-3.123

For the *HO* model space, we have performed calculations by means the HO and KB3G48 interactions with ${}^{48}_{20}$Ca core. The HO interaction of Horie *et al.*, in [38], was built using the two-body matrix elements of the proton-proton interaction taken from the low-lying energy levels of the $N = 28$ nuclei, while those of $\pi(1f_{7/2}) - \nu(2p_{3/2}, 1f_{5/2}, 2p_{1/2})$ interaction have been determined by a least-square fitting to the observed energy spectra of the $N = 29$ isotones. The single-neutron energies for the HO interaction are given in Table 2 [38]. The single-neutron energies of $2p_{3/2},\ 2p_{1/2}$ and $1f_{5/2}$ levels in ${}^{49}_{20}$Ca are determined by the averaging over the level energies of the same spin weighed by the spectroscopic factors of the ${}^{48}Ca(d,p){}^{49}Ca$ reactions [38,39]. The new modified effective interaction KB3G48 is constructed from the microscopic Kuo-Brown's G-matrix interaction KB3GPN [30,31]. This interaction was built using $\pi(1f_{7/2}) - \nu(pf)$ valence space with ${}^{48}_{20}$Ca core. This space model reduces the number of TBMEs into 74 elements. To account for the expected mass dependence of the residual interaction, we have scaled all 74 TBMEs by $(48/40)^{-1/3}$. The values of the neutron SPEs were taken from experiment of the ^{49}Ca spectra [37]. These values are also listed in Table 2. The single-proton energy for $\pi(1f_{7/2})$ is taken from the experimental ^{49}Sc spectra [37].

3. Results and Discussions

The systematic study of the spectroscopic calculations for the neutron rich nuclei even-even ${}_{20}$Ca isotopes with neutron number $30 \leq N \leq 38$ was carried out and the obtained results are compared with the available experimental data [37]. In our study, the valence neutrons occupy the orbits $\nu(1f_{7/2}, 2p_{3/2}, 1f_{5/2}, 2p_{1/2})$ of model spaces *fppn* and *HO* for ${}^{40}_{20}$Ca and ${}^{48}_{20}$Ca neighbors, respectively. Microscopic calculations were performed by means of Nushell code with such interactions as GX1APN, KB3GPN, HO and KB3G48.

Fig. 1 displays the comparison of the obtained results for $E(2_1^+)$ energies of isotopes of ${}^{50-58}$Ca with the available experimental data. One notes that the experimental values are not identified for ^{56,58}Ca isotopes. These energies are used as the first indications of shell structures and their evolution. In general, Fig.1 can obviously show that the calculations lead to agreements in energies with experiment. Moreover, both interactions KB3GPN and KB3G48 have a similar emergence, with a large agreement for $N = 30$ and 32 where the energy difference does not go beyond 380 keV for $N = 34$. However, the large difference between the energy results with HO interaction and the experimental values was observed around $N = 32$ and 34. The large values of $E(2_1^+)$ energy with the interactions KB3GPN and KB3G48 indicate that the sub-shell closure at $N = 32$ is further supported by corresponding low value of the reduced probability $B(E2;\ 2_1^+ \rightarrow 0_1^+)$ in this neutron number. Sub-shell closure at $N = 34$ is predicted for GX1APN and HO interactions with the large values of $E(2_1^+)$ and corresponding low value of $B(E2;\ 2_1^+ \rightarrow 0_1^+)$ as shown in Figs. 1 and 3.

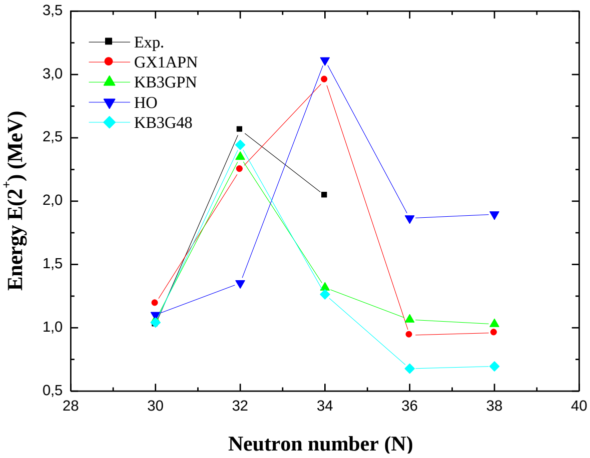

Fig. 1.Comparison of calculated $E(2_1^+)$ energies with the experimental data for neutron-rich Ca isotopes with neutron number $30 \leq N \leq 38$.

According to the results of Ref. [40], the appearance of the new sub-shell closure ($N = 32$ and $N = 34$) in calcium isotopes lies in the mutual arrangement of single-particle states, i.e. that it depends on the gap values of $\Delta_1 = \varepsilon_{\upsilon 2p_{1/2}} - \varepsilon_{\upsilon 2p_{3/2}}$ and $\Delta_2 = \varepsilon_{\upsilon 1f_{5/2}} - \varepsilon_{\upsilon 2p_{1/2}}$. The subshell $N = 32$ occurs if Δ_1 is larger than Δ_2, which presents as the orbit $\nu 1f_{5/2}$ moves upward in energy due to a weakening of the attractive proton-neutron interaction $\pi 1f_{7/2} - \nu 1f_{5/2}$ as protons are removed from the orbit $\pi 1f_{7/2}$. However, the subshell $N = 34$ arises in the opposite case. For the interaction GX1APN, $\Delta_1 = 1.542$ and $\Delta_2 = 2.754$, while for the interaction HO, which also leads to peak of the 2_1^+ energies at $N = 34$, we have $\Delta_1 = 2.028$ and $\Delta_2 = 1.930$. Meanwhile, for the interaction KB3GPN, $\Delta_1 = 2.000$ and $\Delta_2 = 2.500$, we obtain the energy peak at $N = 32$, whereas for the interaction KB3G48, the peak of the 2_1^+ energies appears at $N = 32$, we have $\Delta_1 = 2.023$ and $\Delta_2 = 1.562$. Thus we see that due to the Δ_1/Δ_2 ratio it would be more preferably to have the energy peak and minimal $B(E2)$ values for the KB3GPN at $N = 34$ and energy peak minimal $B(E2)$ at $N = 32$ for the interaction HO. However, calculations lead to the opposite result.

The energy ratio $R_{4/2}$ is one of the most remarkable structural signatures. Besides, the ratio $R_{4/2}$ is one of the few whose absolute value is directly meaningful. For even-even nuclei near shell closures, the value $R_{4/2} < 2$ is characteristic of a near magic, $R_{4/2} \approx 2$ for a spherical-vibrational, $R_{4/2} \approx 2.5$ for a transitional and $R_{4/2} \approx 3.33$ for an ideally symmetric rotor (rigid-rotor) [41]. In Fig. 2, we have shown the $R_{4/2}$ ratios from experimental and calculated results for neutron-rich Ca isotopes by GX1APN, KB3GPN, HO and KB3G48 interactions. Note that the only available experimental values are for ^{50}Ca and ^{54}Ca nuclei. We can clearly see in Fig. 2 that the results of $R_{4/2}$ ratios of the new effective interaction KB3G48 are very closed to the experimental data for ^{50}Ca and ^{54}Ca isotopes, which are around 4.4 and 2.2 MeV, respectively. It is also clear that the data available indicate that the ratio is less than 2.0 $\left(R_{4/2} < 2\right)$ toward a near sub-shell closures character at $N = 32$ with KB3GPN and KB3G48 interactions. Moreover, the other interactions show that the sub-shell closure are at $N = 36$ and 38. According to the self-consistent calculations that use the Gogny interaction [42], all even $^{50-58}$Ca isotopes are spherical ones ($\beta = 0$). Thus, the increase of $R_{4/2}$ ratios in ^{50,52}Ca is due not to deformation but to the feature of the single-particle spectrum.

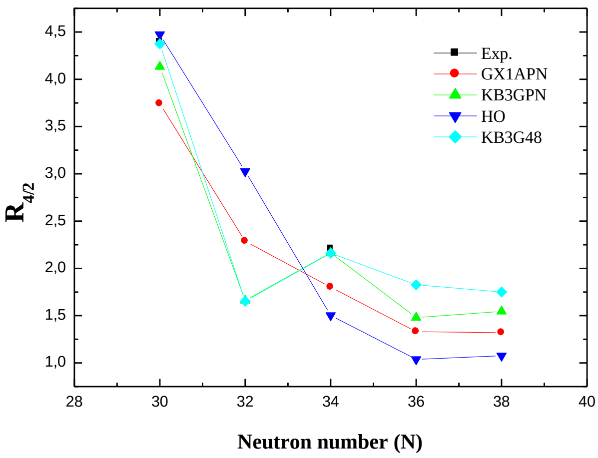

Fig. 2.Comparison of calculated $R_{4/2}$values with the experimental for neutron-rich $^{50-58}Ca$ isotopes.

Following our objective, investigation of the existence of the new sub-shell closure, we also calculated the reduced electric transition probabilities $B(E2;\ 2_1^+ \rightarrow 0_1^+)$. The values of $B(E2;\ 2_1^+ \rightarrow 0_1^+)$ are usually considered as the second important signature of sub-shell closure in even-even nuclei by their smallest values corresponding to the highest energy values of the first excited state 2_1^+. In Fig. 3, the variation of $B(E2;\ 2_1^+ \rightarrow 0_1^+)$ of isotopes of $^{50-58}_{20}Ca$ is shown with neutron number for all the interactions implemented along with the experimental data the effective neutron charge $e_n = 0.45e$.

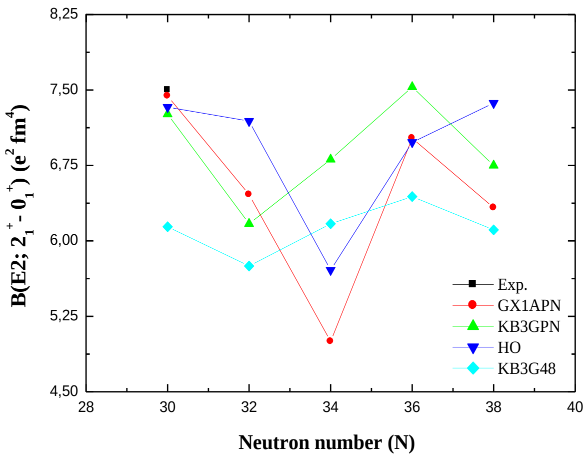

Fig. 3.Comparison of calculated $B(E2)$ values with the experimental data for $^{50-58}Ca$ isotopes. The calculated values are obtained using the effective neutron charge e_n = 0.45e.

We listed in Table 3 the obtained values of $B(E2)$ for transitions, from first 2_1^+ excited state to ground state 0_1^+ and from first 4_1^+ excited state to 2_1^+ state. In the calculations of $B(E2)$, we used two different values of neutron effective charges such as $e_n = 0.50e$ and $e_n = 0.45e$. The present results of $B(E2)$, with GX1APN, KB3GPN, HO and KB3G48 interactions, are compared with experimental data [37,43,44] and the available published ones [44]. Only experimental value in ^{50}Ca isotope is available. One may see that the calculated values of $B(E2)$ depend on the effective charge values. It is clearly shown in Table 3 that the KB3G48 interaction using $e_n = 0.50e$ is close to the experiment. Nevertheless, the resulting outcomes of GX1APN, KB3GPN and HO $e_n = 0.45e$ are too close to the experimental values. Furthermore, our obtained results are in a reasonable agreement with the predictions of other models (*fp*, *IM-SRG*) of Bhoy *et al*., [44] using neutron effective charge 0.50e.

Table 3: Experimental [37,43,44], *theoretical* [44] *and calculated* $B(E2)$ *values (in* e^2fm^4*). Two set of effective charges are implemented:* e_n*=0.5e and* e_n*=0.45e.*

Nuclei	Transition	Exp	GX1APN		KB3GPN		HO		KB3G48		fp	IM-SRG
			e_n=0.5	e_n=0.45	e_n=0.5	e_n=0.45	e_n=0.5	e_n=0.45	e_n=0.5	e_n=0.45	e_n=0.5	
$^{50}Ca_{30}$	$2_1^+ \rightarrow 0_1^+$	7.45	9.18	7.44	8.97	7.26	9.05	7.33	7.58	6.14	7.82	8.00
	$4_1^+ \rightarrow 2_1^+$	≥1.1	12.09	9.79	1.76	1.42	4.00	3.24	2.34	1.89	-	-
$^{52}Ca_{32}$	$2_1^+ \rightarrow 0_1^+$	-	7.98	6.46	7.62	6.17	8.87	7.19	7.10	5.75	6.16	6.46
	$4_1^+ \rightarrow 2_1^+$	-	2.82	2.29	5.02	4.07	5.08	4.12	4.83	3.91	-	-
$^{54}Ca_{34}$	$2_1^+ \rightarrow 0_1^+$	-	6.18	5.00	8.41	6.81	7.05	5.71	7.62	6.17	6.34	6.13
	$4_1^+ \rightarrow 2_1^+$	-	3.58	2.90	5.08	4.12	4.24	3.44	4.92	3.99	-	-
$^{56}Ca_{36}$	$2_1^+ \rightarrow 0_1^+$	-	8.67	7.02	9.30	7.53	8.62	6.98	7.95	6.44	8.95	6.90
	$4_1^+ \rightarrow 2_1^+$	-	4.33	3.51	3.82	3.10	3.23	2.62	4.11	3.33	-	-
$^{58}Ca_{38}$	$2_1^+ \rightarrow 0_1^+$	-	7.81	6.33	8.33	6.75	9.10	7.37	7.54	6.11	8.25	6.85
	$4_1^+ \rightarrow 2_1^+$	-	5.94	4.81	6.00	4.86	6.58	5.33	5.41	4.38	-	-

For most nuclei, both the measurement and the theoretical [45], the values of $B_{4/2} = B(E2;\ 4_1^+ \ \rightarrow\ 2_1^+)/B(E2;\ 2_1^+ \ \rightarrow\ 0_1^+)$ ratio are between $B_{4/2} = 2.0$ and $B_{4/2} = 1.43$ limits of the vibrational and rotational models, respectively. Values of $B_{4/2}$ below 1.0 are certainly possible when the spectrum is dominated by two quasi-particle excitations that are common near magic numbers [45].

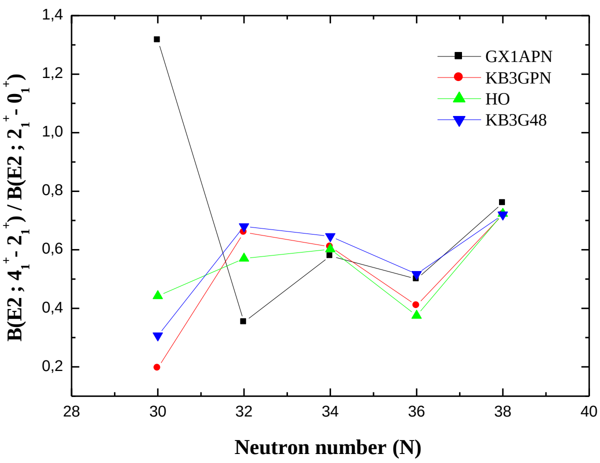

Fig. 4.Calculated values of $B(E2;\ 4_1^+ \ \rightarrow\ 2_1^+)/B(E2;\ 2_1^+ \ \rightarrow\ 0_1^+)$ *for* $^{50-58}Ca$ *isotopes.*

The systematic character of the obtained results of $B_{4/2}$ for the chain of $^{50-58}_{20}$Ca isotopes with neutron number $30 \leq N \leq 38$ using GX1APN, KB3GPN, HO and KB3G48 interactions is shown in Fig. 4. Unfortunately, there are no the available experimental or adopted values in the literature. It should be noted that the ratios of $B_{4/2}$ resulting from the calculated values in $^{52-58}_{20}$Ca are less than 1.0. Hence, they might indicate a close character to the sub-shell closures at $N = 32$ with KB3GPN and KB3G48 interactions, and $N = 38$ with GX1APN and HO interactions in $^{50-58}_{20}$Ca isotopic chain (see Fig. 4). In general, both KB3GPN and KB3G48 interactions give us almost the same results.

4. Conclusion

In this project, the appearance of new shell closures in neutron-rich nuclei even-even $^{50-58}_{20}$Ca isotopes has been studied using the two space models $fppn$ and $\pi(f_{7/2}) - \nu(pf)$ with $^{40}_{20}$Ca and $^{48}_{20}$Ca cores, respectively. The microscopic calculations have been performed by means of Nushell code with phenomenological interactions. Furthermore, some modifications have been made in the original interaction KB3GPN to get a new interaction called KB3G48. The results of our theoretical calculations GX1APN, KB3GPN and KB3G48 have been compared with the available experimental data. A very good agreement was obtained for ^{50,52}Ca nuclei. However, the calculated $E(2_1^+)$ energies with HO interaction were so different from the experimental data. The experimental values of $E(2_1^+)$ energies are not available for ^{56,58}Ca nuclei. The calculated values, with two values of neutron effective charge, were very similar and in good agreement with experiment for most transitions in $^{50}_{20}$Ca isotope. Based on the calculated values of the spectroscopic parameters $E(2_1^+)$ and $B(E2)$, we have reproduced the new magic numbers $N = 32$ in $^{52}_{20}$Ca with KB3GPN and KB3G48 interactions and $N = 34$ in $^{54}_{20}$Ca with GX1APN and HO interactions. Moreover, the calculated values of the ratios $R_{4/2}$ of the excitation energies and $B_{4/2}$ of the reduced transition probabilities indicate that the sub-shell closures are at $N = 36$ and 38 with GX1APN and HO. Both $R_{4/2}$ and $B_{4/2}$ spectroscopic parameters give us the same new magic numbers $N = 32$ in $^{52}_{20}$Ca with KB3GPN and KB3G48 interactions.

Finally, the experimental data have been well described by the new interaction KB3G48. Wherever data does not exist, our results will possibly provide predictions of unexplored properties of neutron-rich calcium isotopes.

Acknowledgements

The authors extend their special thanks to B. A. Brown for his help in providing the OXBASH and the NUSHELL@MSU codes (Windows version).

References

[1] M.G. Mayer and J.H.D. Jensen, Elementary Theory of Nuclear Shell Structure, Wiley, New York, (1955).

[2] E. Caurier, G. Martínez-Pinedo, F. Nowacki, A. Poves and A.P. Zuker, Rev. Mod. Phys. 77(2), 427 (2005) ; https://doi.org/10.1103/RevModPhys.77.427

[3] B. A. Brown and W.D.M. Rae, The shell-model code NuShellX@MSU, Nucl. data sheets 120, 115-118 (2014) ; https://doi.org/10.1016/j.nds.2014.07.022

[4] M.G. Mayer, Phys. Rev. 75, 1969-1970 (1949) ; https://doi.org/10.1103/PhysRev.75.1969

[5] O. Haxel, J. H. D. Jensen and H. E. Suess, Phys. Rev. 75, 1766 (1949) ; https://doi.org/10.1103/PhysRev.75.1766.2

[6] T. Motobayashi, Y. Ikeda, Y. Ando, K. Ieki, M. Inoue et al., Phys. Lett. B 346, 9 (1995) ; https://doi.org/10.1016/0370-2693(95)00012-A

[7] C.C.M. Campbell, N. Aoi, D. Bazin, M. D. Bowen, B. A. Brown et al., Phys. Rev. Lett. 97(11), 112501(4) (2006) ; https://doi.org/10.1103/PhysRevLett.97.112501

[8] B. Bastin, S. Grévy, D. Sohler, O. Sorlin, Zs. Dombrádi et al., Phys. Rev. Lett. 99(2), 022503 (2007) ; https://doi.org/10.1103/PhysRevLett.99.022503

[9] D. Steppenbeck, S. Takeuchi, N. Aoi, P. Doornenbal, M. Matsushita et al., Phys. Rev. Lett. 114(25), 252501 (2015) ; https://doi.org/10.1103/PhysRevLett.114.252501

[10] A. Huck, G. Klotz, A. Knipper, C. Mieh, C. Richard-Serre, Walter, A. Poves, H. L. Ravn, and G. Marguier, Phys. Rev. C 31(6), 2226 (1985) ; https://doi.org/10.1103/PhysRevC.31.2226

[11] F. Wienholtz, , D. Beck , K. Blaum , Ch. Borgmann , M. Breitenfeldt et al., Nature 498, 346 (2013) ; https://doi.org/10.1038/nature12226

[12] R.V.F. Janssens, B. Fornal, P.F. Mantica, B.A. Brown, R. Broda et al., Phys. Lett. B 546, 55 (2002).

[13] S. N. Liddick, P. F. Mantica, R. Broda, B. A. Brown, M. P. Carpenter et al., Phys. Rev. C 70(6), 064303 (2004).

[14] B. Fornal, S. Zhu, R. V. F. Janssens, M. Honma, R. Broda et al., Phys. Rev. C 70, 064304 (2004).

[15] A. Goldkuhle, C. Fransen, A. Blazhev, M. Beckers, B. Birkenbach et al., Phys. Rev. C 100(5), 054317 (2019).

[16] J.I. Prisciandaro, P.F. Mantica, B.A. Brown, D.W. Anthony, M.W. Cooper et al., Phys. Lett. B 510, 17 (2001) ; https://doi.org/10.1016/S0370-2693(01)00565-2

[17] A. Bürger, T.R. Saito, H. Grawe, H. Hübel, P. Reiter et al. , Phys. Lett. B 622, 29 (2005).

[18] M. Rosenbusch, P. Ascher, D. Atanasov, C. Barbieri, D. Beck et al., Phys. Rev. Lett. 114, 202501 (2015) ; https://doi.org/10.1103/PhysRevLett.114.202501

[19] X. Xu, M. Wang, K. Blaum, J. D. Holt, Yu. A. Litvinov et al., Phys. Rev. C 99 (6), 064303 (2019) ; https://doi.org/10.1103/PhysRevC.99.064303

[20] M. P. Reiter, S. Ayet San Andrés, E. Dunling, B. Kootte, E. Leistenschneider et al., Phys. Rev. C 98(2), 024310 (2018) ; https://doi.org/10.1103/PhysRevC.98.024310

[21] D. Steppenbeck, S. Takeuchi, N. Aoi, P. Doornenbal, M. Matsushita et al., Nature 502, 207 (2013) ; https://doi.org/10.1038/nature12522

[22] S. Chen, J. Lee, P. Doornenbal, A. Obertelli, C. Barbieri et al., Phys. Rev. Lett. 123(14), 142501 (2019).

[23] H. N. Liu, A. Obertelli, P. Doornenbal, C. A. Bertulani, G. Hagen et al., Phys. Rev. Lett. 122(7), 072502 (2019) ; https://doi.org/10.1103/PhysRevLett.122.199602

[24] G. Hagen, M. Hjorth-Jensen, G.R. Jansen, R. Machleidt and T. Papenbrock, Phys. Rev. Lett. 109(3), 032502 (2012) ; https://doi.org/10.1103/PhysRevLett.109.032502

[25] H. Hergert, S.K. Bogner, T.D. Morris, S. Binder, A. Calci, J. Langhammer and R. Roth, Phys. Rev. C 90 (4), 041302 (2014) ; https://doi.org/10.1103/PhysRevC.90.041302

[26] S. Michimasa, M. Kobayashi, Y. Kiyokawa, S. Ota, D.S. Ahn et al., Phys. Rev. Lett. 121(2), 022506 (2018) ; https://doi.org/10.1103/PhysRevLett.121.022506

[27] W.A. Richter, MG. V. Der Merwe, R.E. Julies and B.A. Brown, Nucl. Phys. A 523(2), 325 (1991) ; https://doi.org/10.1016/0375-9474(91)90007-S

[28] A. Poves, J. Sánchez-Solano, E. Caurier, and F. Nowacki, Nucl. Phys. A 694, 157 (2001) ; https://doi.org/10.1016/S0375-9474(01)00967-8

[29] M. Honma, T. Otsuka, B. Brown and T. Mizusaki, Eur. Phys. J. A 25, 499 (2005) ; https://doi.org/10.1140/epjad/i2005-06-032-2

[30] A. Poves and A. P. Zuker, Phys. Rep. 70(4), 235 (1981) ; https://doi.org/10.1016/0370-1573(81)90153-8

[31] T. T. S. Kuo and G. E. Brown, Nucl. Phys. A 114, 241 (1968) ; https://doi.org/10.1016/0375-9474(68)90353-9

[32] M. Honma, T. Otsuka, B. A. Brown and T. Mizusaki, Phys. Rev. C 65(6), 061301 (2002) ; https://doi.org/10.1103/PhysRevC.65.061301

[33] M. Hjorth-Jensen, T. T. S. Kuo and E. Osnes, Phys. Rep. 261, 125 (1995) ; https://doi.org/10.1016/0370-1573(95)00012-6

[34] H. L. Cohen, R. H. Fulmer, A. I. McCarthy and D P. Mukherjee, Rev. Mod. Phys. 35, 332 (1963) ; https://doi.org/10.1103/RevModPhys.35.332

[35] V. Gillet and E. A. Sanderson, Nucl. Phys. 54, 472 (1964); https://doi.org/10.1016/0029-5582(64)90427-4

[36] M. Honma, T. Otsuka, B. A. Brown and T. Mizusaki, Phys. Rev.C 69, 034335 (2004) ; https://doi.org/10.1103/PhysRevC.69.034335

[37] Data extracted using the NNDC On-line Data service from the ENSDF database, http://www.nndc.bnl.gov/ensdf/; file revised as of April 01, 2021.

[38] H. Horie and K. Ogawa, Prog. Theor. Phys 46(2), 439(1971) ; https://doi.org/10.1143/PTP.46.439

[39] E. Kashy, A. Sperduto, H. A. Enge and W. W. Buechner, J. Exp. Theo. Phys. 135, B865 (1964) ; https://doi.org/10.1103/PhysRev.135.B865

[40] T. Otsuka, A. Gade, O. Sorlin, T. Suzuki and Y. Utsuno, Rev. Mod. Phys. 92, 015002 (69) (2020) and arXiv:1805.06501 (2020) ; https://doi.org/10.1103/RevModPhys.92.015002

[41] M.M. Hammad, M.M. Yahia and S.B. Doma, https://hal.archives-ouvertes.fr/hal-02268933/ (2019).

[42] http://www-phynu.cea.fr/HFB-Gogny_eng.htm

[43] D.Montanari, S.Leoni, D.Mengoni, J.J.Valiente-Dobon, G.Benzoni, N.Blasi et al., Phys. Rev. C 85(4), 044301 (2012).

[44] B. Bhoy, P. C. Srivastava and K.Kaneko, https://arxiv.org/abs/1906.00706v3 (9), (2020).

[45] J.P. Delaroche, M. Girod, J. Libert, H. Goutte, S. Hilaire, S. Péru, N. Pillet and G.F. Bertsch, Phys. Rev. C 81(1), 014303 (2010) ; https://doi.org/10.1103/PhysRevC.81.014303